

Increasing Spatial and Directional Accuracy for the Dimensioning Drag Loads from Accidental Explosions

Nicolas Salaün^a, Lars Rogstadkjernet^a, Per Erik Nilsen^b, Djurre Siccama^a

^a Gexcon (Gexcon AS, Fantoftvegen 38, NO-5072 Bergen, Norway); ^b Statoil ASA, Bergen, Norway

E-mail: nicolas@gexcon.com

In an industrial explosion, different objects will be exposed to different types of loading where smaller equipment is primarily affected by drag loads (also called dynamic pressure, as opposed to the explosion incoming static overpressure). Advanced modelling tools such as the FLACS CFD tool are widely used and provide detailed description of explosion loading. Drag loads typically display large spatial variations but are commonly simplified to a single conservative load value when used as design basis. This implies a substantial cost penalty and gives no incentive for the engineer to arrange equipment in a manner that reduces exposure. Design challenges often arise when small equipment is defined as safety critical. In this paper, more accurate ways to identify and report dimensioning drag loads are presented. Such improvement in drag load definition will help piping engineers to improve blast resistant design and avoid excessive design measures in low risk process areas. Cost effectiveness is increased as investments spent on high structural strengths are limited to the areas where it is needed.

An illustrative case from an offshore module is presented to demonstrate the problem and solutions. This paper explores various ways to identify and report drag loads. Key focus is increased spatial accuracy and how this information can be presented in a manner useful for the designing engineers. The directional components of the absolute drag are also explored to demonstrate how it can support an optimized design.

Proper definition of design load is a major topic in development project and CFD explosion analyses commonly performed as part of the QRA. Hence, in most projects the information required for targeted design is easily available. In projects with high drag loads, refining drag load distribution is likely to achieve safe-equivalent designs at lower cost.

Keywords: *industrial explosions, drag loads, spatial distribution, directional loading, safety critical elements, small objects, FLACS-risk*

Introduction

For installations with severe explosion hazards, Dimensioning Accidental Loads (DALs) are identified in Explosion Risk Analysis (ERA) performed in compliance with industrial standards (NORSOK Z-013, 2010), (ISO 19901-3, 2010)...). These analyses are supported by advanced 3D CFD (Computational Fluid Dynamics) modelling tools such as the FLACS software. CFD provides detailed description of pressure loads resulting from accidental explosions. As the resulting force experienced by an object subject to gas explosion depends on its size and on the relative contribution between the effects of the overpressure wave and of the dynamic flow, CFD results are usually differentiated between static overpressure and dynamic pressure (drag). Drag is the main type of loads affecting small-bore objects. Design requirements for smaller equipment and piping are based on drag. Conventional probabilistic risk analysis identifies these DALs which are later used for the design and/or response assessment. The DAL for drag represents the probabilistic absolute drag value exceeded at a specific return frequency. Commonly, a generic 10^{-4} pr. year return criteria is used based on the deemed acceptable escalation risk following an explosion.

In today's practice, DAL for drag is typically reported as a single "generic" value per "area of interest". The historical basis for this format is that strength requirement for piping and small pieces of equipment can then be derived from a single exceedance chart and that frequency of failure and design criteria can be identified from the same chart. Although practical and perhaps sufficiently detailed from a risk perspective, this way of reporting drag loads under communicates and obscures the highly diversified nature of drag loading. It disregards the large span in loads between different areas and it gives no guidance on what areas will see high and low drag loads. This way of representation gives no constructive recommendation when positioning drag sensitive equipment units, nor does it present any information on the directional loading of these items. In consequence, all items are designed to the same standard. This will inherently mean excessive conservative design requirements in some areas with little or no credit given to "clever" pipe routing.

The purpose of this paper is to illustrate methods and benefits of deriving more adequate and cost effective DAL for drag. The methodology is illustrated through an example of an actual study of a large North Sea platform. The drag loads are reported with increased accuracy using the detailed information already available in the original analysis and minimal additional work. The first focus of the paper is to provide a better understanding of the drag loads and to demonstrate spatial nature of drag due to the module characteristics. A main feature of the presented methodology is to avoid oversimplification of the spatial distribution of drag while still maintaining consistency with conventional practices. It is considered particularly useful when defining design strength requirements but it also provides practical information to the designing engineers. A notable improvement is that engineers will be enabled to optimise equipment location and avoid routing piping in high drag areas. The method also quantifies the reduction in strength requirements arising from a "better" assessment, defines dimensioning loads, and helps checking integrity of safety functions... The second focus is the directional dependency of the drag loads and how this information can be useful to understand the prevailing directional loading mode in order to support an optimized design.

The FLACS CFD code

FLACS is a commercial Computational Fluid Dynamics (CFD) code developed by GexCon to model the dispersion and combustion of flammable materials in large 3D geometries. FLACS is the industry standard for CFD explosion modelling in the Oil and Gas industries. It is increasingly used in the nuclear industry. Current capabilities also include flammable and toxic gas dispersion, pool spread and evaporation of liquefied gases (e.g. LNG). Latest improvements include a fire and heat load simulation solver (FLACS-Fire). Using 3D CFD to predict the consequences of hazardous scenarios, all contributing protective measures (ventilation, deluge, gas detection, confinement, physical protections...) can efficiently be taken into account increasing predictions accuracy. This paper takes advantage of the FLACS capabilities to simulate gas explosion and to assess the resulting transient loading distribution.

Signification of drag and related potential improvements in the reporting of drag

Drag (loads) from FLACS

An important distinction when dealing with drag is the difference between loading and actual force exerted onto an object. For safety engineers, drag is commonly expressed as a load, and is analogue to an overpressure load. In practical terms, drag as provided by FLACS, is representative for the “wind” of the explosion. It is indistinctively named drag load, drag pressure, dynamic pressure... It refers to an absolute value and is expressed as in Equation (1):

$$DRAG [Pa] = \frac{1}{2} \times \rho [kg/m^3] \times V [m/s]^2 \quad (1)$$

As the expression of absolute drag is related to the absolute velocity V, there is a large span of drag values across the module i.e. high spatial dependency. There are 3-components of the drag, each of them being related to the associated projection of the velocity vector in the Cartesian domain used in FLACS: DRAG_x, DRAG_y and DRAG_z. Finally, drag is a transient load that can be expressed as drag (t); the former applies to all components DRAG_x(t), DRAG_y(t), DRAG_z(t).

Using CFD and FLACS in particular, several ways are available to monitor drag related variables. Absolute drag, DRAG_x, DRAG_y and DRAG_z can be assessed independently. Exact approaches depend on established practises in different consultancy companies. In order to access time history of output parameters and to consider spatial accuracy, GexCon’s standard way of reporting drag related output uses monitoring points located in the control volumes from the FLACS mesh. Monitoring points track parameters with time and provide transients whereas 3D / volume monitoring will report the maximum over time at periodic intervals only.

Deriving drag forces from drag loads

For piping/structural engineers, what matters are the actual forces (and response) resulting from explosion loads. Explosion loads are commonly expressed as static (differential) overpressure loads, drag loads and combination of these two, principally. The total force experienced by an object located in an explosion will result from the sum of all the different types of transient loadings. The size of the object (practically when using CFD, the ratio of the object size versus the grid cell size) will determine what load type is dominant. It is commonly accepted that small bore objects are affected mostly by drag, whereas for large objects the overpressure difference between the object sides is preponderant.

For a small object enduring a drag load, the consequential drag force results from the aerodynamic interaction between the flow and the object. Hence, the force will depend on the size and shape of the object and on how the object is placed within the explosion flow field. Similar objects of different sizes will experience different drag forces (e.g. a pipe with or without insulation). An oriented object will experience different drag forces (e.g. sections of a pipe travelling in 3D inside the module, a horizontal cylindrical reservoir, a pump...) for different flow fields. The following Equations (2) express the force resulting from the drag load:

$$\begin{aligned} FORCE_{DRAG}(t) &= \frac{1}{2} \times \rho(t) \times V^2(t) \times C_D \times W_A \\ &= DRAG(t) \times C_D \times W_A \end{aligned} \quad \left| \begin{array}{l} C_D: \text{drag coefficient (-)} \\ W_A: \text{windage area (m}^2\text{)} \end{array} \right. \quad (2)$$

References from the literature provide simplistic empirical values for the aerodynamic coefficient C_D (Baker, 1983); (FABIG, 2005)) assuming simple shapes entirely engulfed in laminar flows or arrangement of several of these elementary shapes. The drag coefficient, C_D represents the fact that some shapes are more or less resistant to a flow. As a simplification no time nor temperature dependency is detailed for C_D. The windage area W_A is defined as a projected surface / shadow area resisting to the flow. The common formulation expresses the maximum force resulting from the explosion over time. Velocity and drag transients can be used to derive the variation of the resulting force with time. One can also highlight that the drag forces will not be uniform towards the 3 directions in space for a given object exposed to a given explosion flow field.

As drag loads varies with time, the same applies to the resulting force. The common response calculation approaches use static equivalent methods where only the maximum absolute drag value over time is used. As a result, the static equivalent FORCE_{DRAG} has to account for a dynamic factor called the Dynamic Load Factor (DLF), applied in equation (2). This DLF expresses the fact that the dynamic response of the studied object may be amplified or insensitive to the transient aspect of the loading depending on its mechanical and constructive properties. It accounts for the fact that a dynamic load can have a significantly larger / lower effect than a static load of the same magnitude due to the structure's inability / aptitude to respond quickly / slowly to the loading (deflecting). The DLF value (between 0 and ~ 2) is related to the duration of the load pulse, t_d, compared to the fundamental period of vibration of the system (1st Eigen period), T.

Keeping in mind these expressions of the drag load and resulting force, recommendations can immediately be suggested to qualitatively reduce vulnerability against drag: pipes should be routed in areas where explosion induced flow are expected to be low (hide behind main structure, ...), avoid routing pipes across main vent paths, to the degree possible align pipe orientation with flow direction, keep in mind orders of magnitude of drag load durations when assessing DLF for drag loads. The above are common recommendations in ERA but (very) little effort is given to detail where these effects occur or their magnitude. Improving the engineering basis for designing against drag loads would include:

- spatial distribution of load magnitude (absolute value);
- spatial distribution of load direction (vector values).

Indeed, in a design stage, the way of reporting drag loads using a single value (i.e. not spatial dependency nor directional dependency) is practical: all items in a given deck is designed to the same standard. However this approach is highly simplistic and gives no constructive recommendation when positioning drag sensitive equipment units nor does it presents any information on the directional loading of these items. This will inherently mean excessive conservative design requirements in some areas with little or no credit given to “clever” pipe routing.

Using specific design loads for different areas or units will in some situation be impractical and potentially costly. In a situation where explosion risk is low there will be little to gain by having differentiated DAL. The benefit would primarily be in installations where drag is high and where designing against these loads involve a high premium. In these situations, improved accuracy of drag load calculations may translate in a severe design load reduction and substantial cost and weight savings.

The following sections deal with reporting refinement and provide examples based on an application upon an offshore module.

Practical application, case study

Geometry & numerical model supporting the study

The offshore gas processing module of interest is 42 m long, 17 m wide and 14 m high (over two levels, platted). For brevity only the lower main deck of the module is included. It is a tunnel-shaped module provided with firewalls on each of the long sides and a combination of openings, louver panels, explosion relief panels and grated weather cladding on the shorter sides. The module is congested with pumps, piping, vertical and horizontal vessels and with a large enclosed volume on the north-western side. Figure 1 is illustrating the corresponding FLACS model. North is along the +Y axis. A large number of monitoring points is distributed over the module (Figure 2). A matrix of 6 (along x-axis) x 22 (along y-axis) x 3 (z-axis) and 9 additional (i.e. 405) monitoring points is used. Each monitoring point covers a volume of 3 x 3 x 2 m.

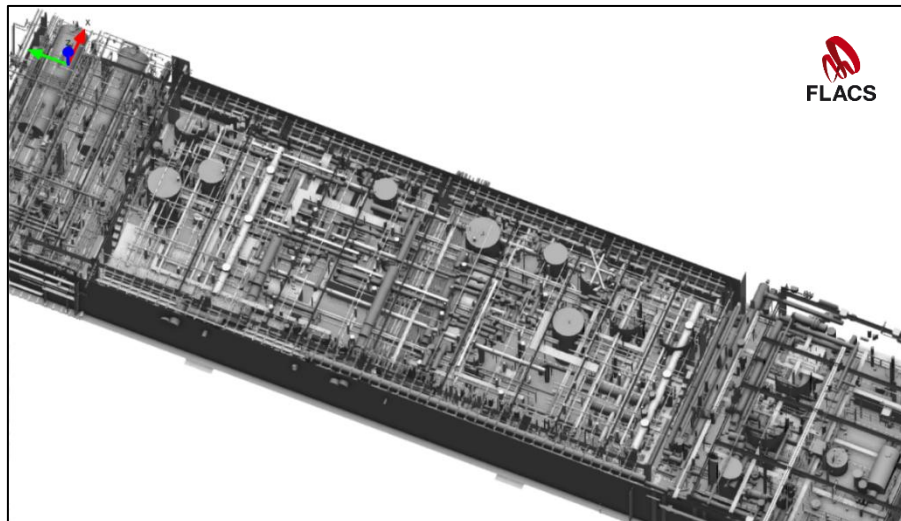


Figure 1: FLACS model used to perform the analysis, upper deck removed for visual purposes

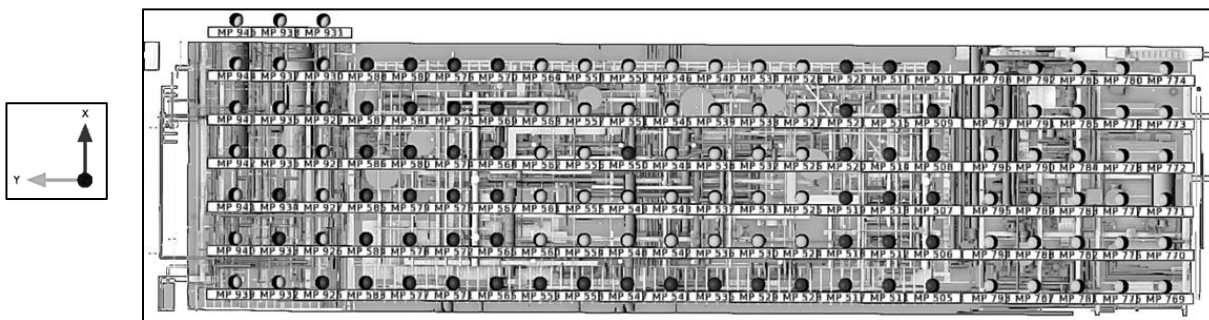


Figure 2: Monitoring points from the FLACS model (top view, 3 layers superimposed)

Explosion Risk Assessment (ERA) & common single «generic» DAL value

Explosion studies for offshore facilities will normally be performed according to (ISO 19901-3, 2010) and (NORSOK Z-013, 2010) estimating the 10^{-4} pr. year DAL. The latter was used for drag in the studied module. A similar example is described in (Davis, et al., 2011). An extensive set of FLACS simulations is performed covering natural ventilation, time-dependent flammable gas clouds dispersion and idealized gas clouds explosion related to identified and quantified risk contributors. For the studied module, approximately 1000 CFD simulations are run, out of which 15 % relate to explosions. The predicted heterogeneous explosive clouds are idealized as equivalent homogeneous clouds (Hansen, et al., 2013) and are ignited at several locations. The simulation work combines with leak frequencies and ignition probabilities to derive a probabilistic description of the resulting maximum drag loads over the entire deck (and over time) for the set of explosion simulations. Figure 3 shows the resulting drag exceedance curve which is in line with common reporting format. Based on the “ 10^{-4} criteria”, the analysis predict a DAL for drag load of 0.69 barg.

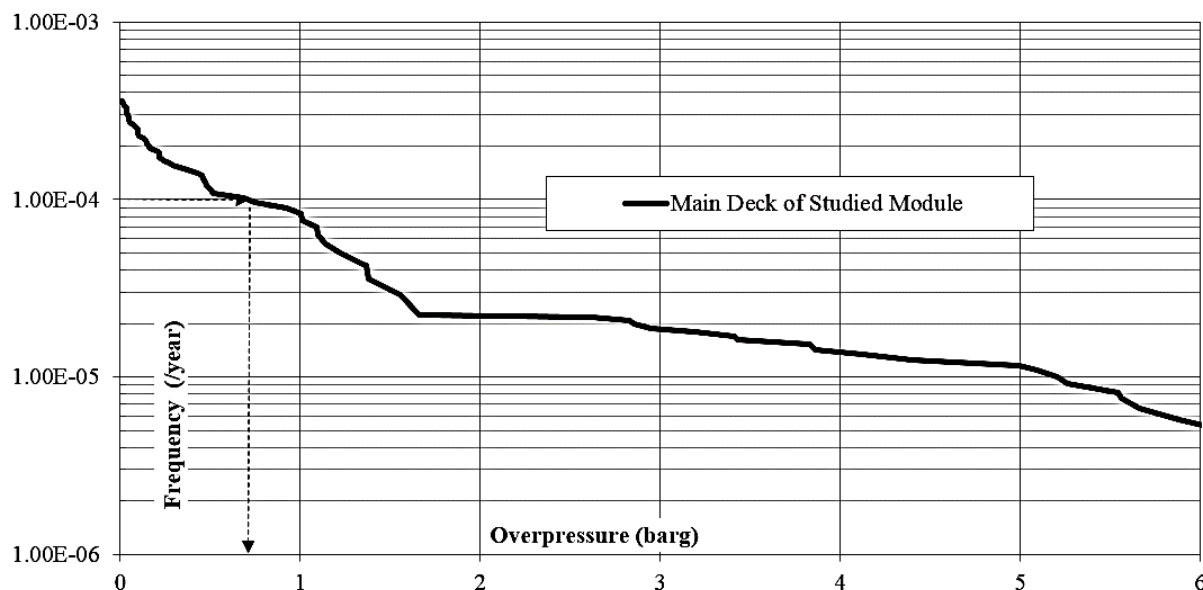


Figure 3: Explosion risk exceedance for drag in the module of interest. The reported DAL (10^{-4} pr. year) is 0.69 barg

Increasing spatial accuracy

Design load requirements are typically based on the idea that escalation is to be prevented at a design stage. As a result, safety critical elements and their supports, must withstand blast loads with a certain return frequency. This criteria relates to the concept of failure in ANY pipe in the module and the sum of all events that can cause pipe failure.

As a consequence the outcome is presented as a single value for the dimensioning drag load for the whole module. However, certain areas may never see high loads. Hence, one may be tempted to reason that dimensioning drag loads could be calculated based on the frequency of load exposure at individual locations (or over subdivided volumes of the deck). The approach for spatially refining loads in an area needs to take account of the fact that there will be spatial variance – while also aligning with the concept of design load based on sum event frequency or the frequency of failure of ANY pipe in order to prevent escalation. The concepts of “exceedance” and retrieving design values at a given fixed criteria make it far from trivial to assess the combined frequency of load or failure of multiple targets when merging individual locations all together.

An essential feature of an ERA is to account for the sum of frequencies for an event. The basis for conventional reporting of DAL is well founded and it is good basis to argue that the magnitude of the drag load with a “single value” approach should be maintained. This principle assures that the combined frequency of load or failure of all targets are accounted for. The load predicted with conventional methodology is hence considered an appropriate load for the most exposed area. A key argument in this paper is that it is not representative for all exposed areas and hence the spatial distribution should be taken into account in engineering and decision making.

Spatial dependency can be achieved by combining the magnitude of the ERA prediction (0.69 barg) with the spatial distribution established through individual probabilistic calculations and exceedance charts for each location of the monitoring points from Figure 2. The results assessed for individual locations are normalized with the maximum peak drag load over the entire module. Peak drag load provided by conventional ERA methodology is representative for the most exposed areas (the most exposed pipe will need to be designed against a force derived from this drag load). The dimensioning criteria is used to derive the relative distribution of dimensioning loading. Consistency with DAL for drag load from the ERA “single value” is maintained, with a further refinement of spatial distribution. From this exercise, the appropriate load for a specific target can be extracted.

Eventually, results are presented in Figure 4 for three elevations in the module. The rows/columns are tagged to help identifying coordinates inside the module. An illustrative colour coding is used to highlight the most / least exposed regions. Blocked regions are highlighted to support understanding and illustrate locations where large objects contribute to flow acceleration.

Directional dependency

The directional components of the absolute drag, $DRAG_x(t)$, $DRAG_y(t)$ and $DRAG_z(t)$ can be extracted independently without any additional effort and allow a more detailed assessment of drag loading. Each parameter can be processed to derive exceedance charts, either on a module basis or on an individual location basis. In a refined exercise, the spatial distribution of the DAL for absolute drag load is compared to 3 sub-plots covering DALs for $DRAG_x$, $DRAG_y$ and $DRAG_z$ originating from individual exceedance curves. In other words, for each and all individual locations, a separate exceedance curve is calculated for the directional drag components. Ultimately, this output give additional information of drag direction as well as spatial distribution. For a given location, maximum values may occur for different instant in time that is why $DRAG_x$, $DRAG_y$ and $DRAG_z$ shall be studied independently and not derived from the maximum absolute drag.

For tunnel shaped modules like the one studied here, expectations are that drag loads occur predominantly along the module axis ($DRAG_y$ component). This implies that the absolute value of drag would more or less coincide with the value found along one of the axis. Such information would have practical implications in design and structural engineers could take advantage of it when designing / checking pipe supports. When designing a pipe following the main axis, constraints to consider for the design (vertical loads $DRAG_z$ and normal loads $DRAG_x$) may be dramatically reduced, thereby removing a significant portion of over conservatism (or steel) and allowing for “clever” pipe routing in a quantified way.

With more open modules, absolute drag values would not be expected to match any of the projected vector values: high drag load could occur in any directions depending on the explosion scenario. Theoretically, in an entirely unconfined situation, drag load components would be equally large and equally likely in all directions. In real configurations, the method ability to determine the governing drag direction becomes of significant interest. Objects exposed to drag would need to withstand a “reduced” loading spread among all directions. There would be no gains to be achieved by smarter design (reorienting objects would not change the loading they experience). The benefit will be a reduced design value compared to absolute drag. Presenting ratio or percentage could also be a way to illustrate prevailing loading directions. For practicality, Gexcon has chosen to maintain the presentation of the results using the loads since values would preferentially be used by structural engineers. Also, for regions of the module where drag loads are on the same magnitude in 2 main directions (which will tend to reproduce what would happen in more open modules), the resulting angled loading can be assumed by comparing the projected contributions with the absolute value.

Knowing the direction of loading is primarily of interest in the high load regions. Hence, results from the studied case are provided for each and every individual locations in Figure 5 for the particular elevation of 1 m above the deck. In other words, the load mapping extracted from the absolute drag output at 1 m elevation in Figure 4 is compared with the DAL for the $DRAG_x$, $DRAG_y$ and $DRAG_z$ components output in Figure 5.

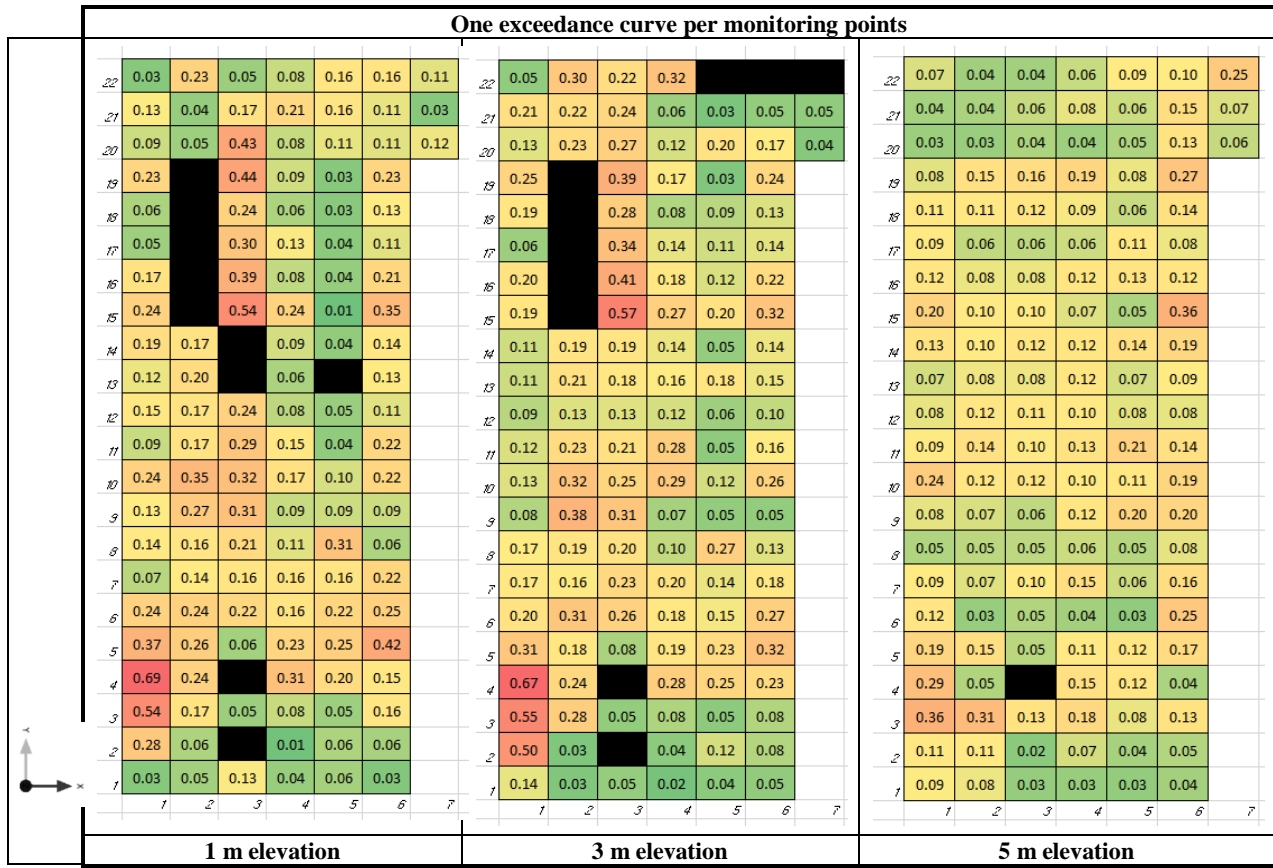


Figure 4: Spatial DAL for absolute drag load distributions to an overall 10^{-4} return frequency for rupture of any pipe in the entire deck. One may note the 0.69 value being the DAL suggested for the whole area based on conventional approach

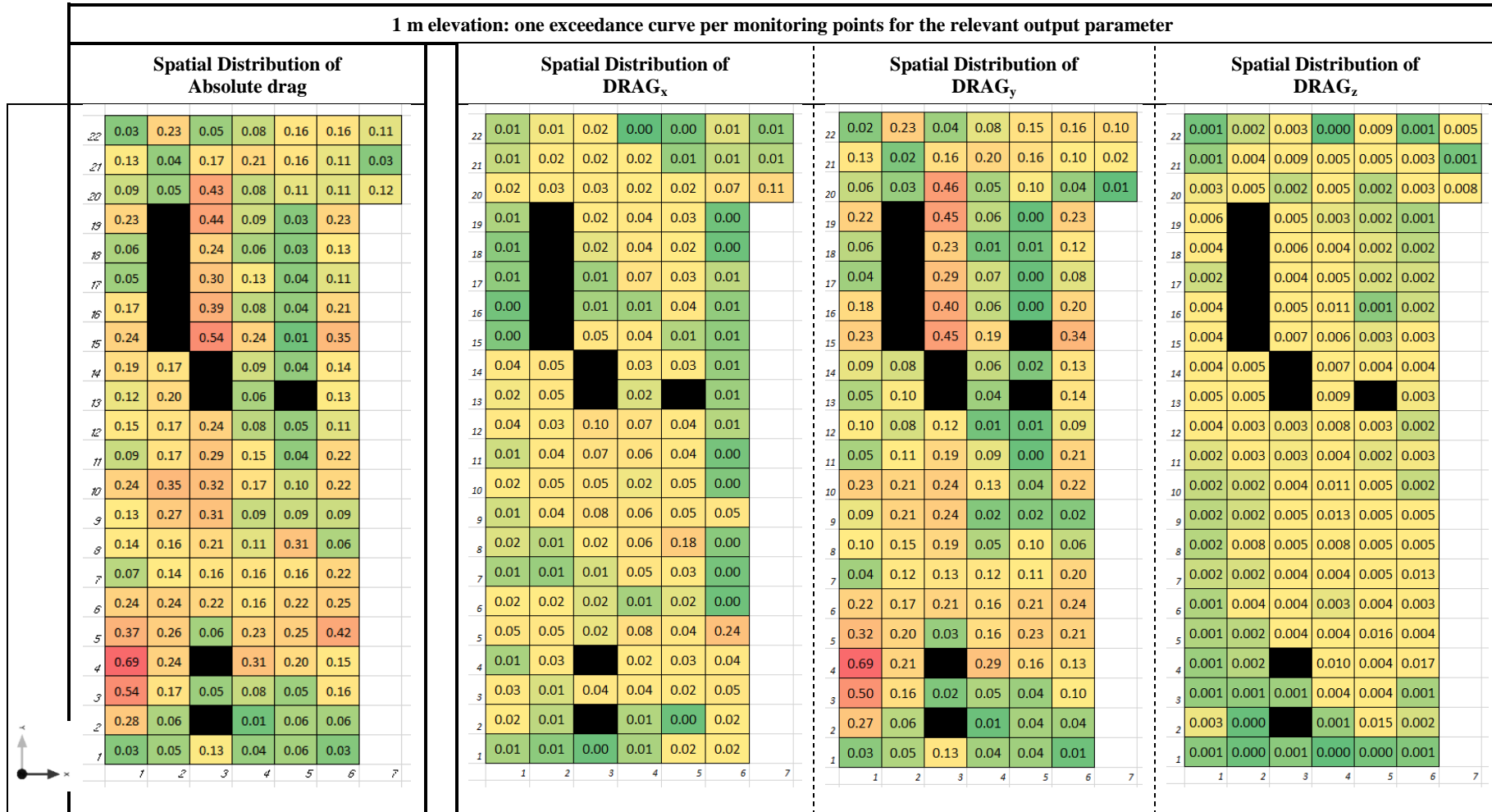


Figure 5: Split of spatial DAL equivalent to overall 10^{-4} return frequency for absolute drag load distributions into directional components $DRAG_x$ (normal), $DRAG_y$ (along module axis) and $DRAG_z$ (vertical) at 1 m elevation. One may note the reference value of 0.69 resurfaces among the $DRAG_y$ values as flow is practically fully aligned with the y axis.

Discussion

Increasing spatial accuracy

A primary objective of this paper has been to increase the understanding of the spatial nature of drag loading which in turn will support more rational and appropriate measures when designing against drag loads. The results from Figure 4 demonstrate a large span in dimensioning drag loads depending on the location: a 1:30 ratio is observed between the most and least exposed areas. Mean values over the whole module are in the range of 20 to 30 % of the maximum value. The presented method explicitly identifies regions where the drag loading is at its maximum and where a special attention needs to be paid. Areas with high drag load are indicated in Figure 6 and demonstrates that large objects, blockages, congested areas have substantial effect on drag loading. 2 specific areas only reports values that are in the magnitude of the maximum value (0.69 barg). The first one is located on the south-west section of the module and covers 7 to 9 volumes from the individual mapping (~ 150 m³). The second one is located on the north-west part at the immediate vicinity of a large enclosed obstacle and covers roughly 180 m³. Compared to the ~ 7 000 m³ of the module itself, this two high drag regions represents ~ 2.2 % of the module.

Eventually, when using a coarser spatial accuracy, the level of details tends to decrease and the conservatism to increase as the number of individual locations is reduced. Compared to this more informative and efficient presentation of the results, the sharpness of the information is somewhat lost for the existing extreme case reporting a “single value”.

Eventually, it is suggested to define the individual location way of reporting as a new standard approach.

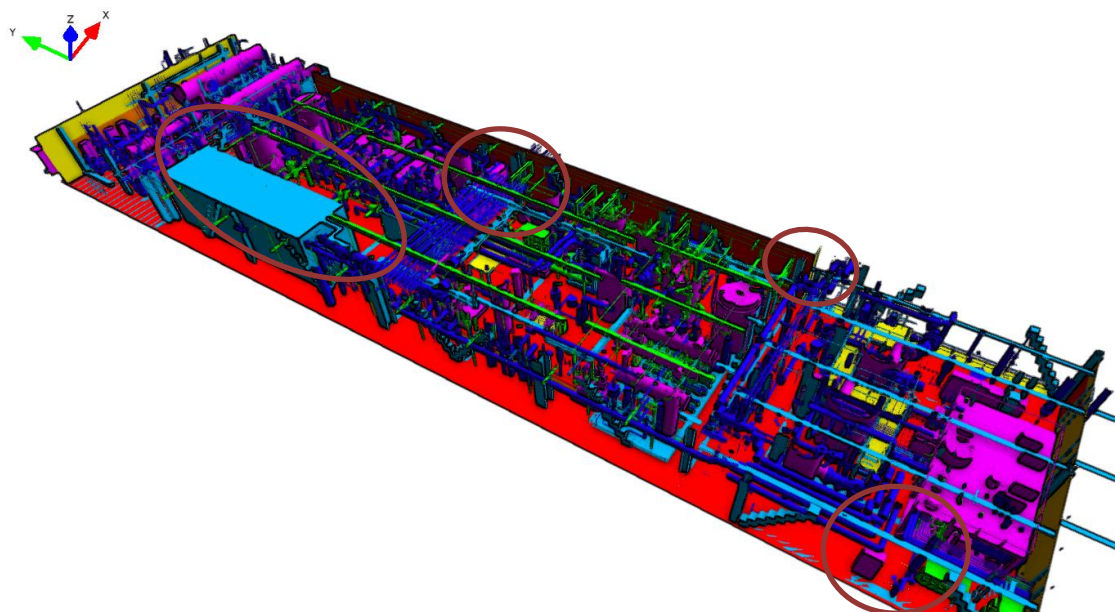


Figure 6: Internal of main deck seen from top, west. Circled areas contributes to increase drag loads

A practical way to present these results is a key factor to make this approach useful for the risk owner and for design engineers.

Hence, a development effort has been started to include this functionality directly in the visualisation post-processor of the software. One of the latest internal development versions of FLACS (FLACS-Risk) makes it possible to superimpose the outcomes of the probabilistic combination over the module geometry. This feature is available through the post processing tool of FLACS and brings a significant added-value in terms of communication of the results, as far as spatial dependency is concerned. The work reported previously as a scalar value at a “monitoring point level” is performed graphically at a “grid size level” (0.25 m definition here).

This feature enables graphical 3D representations of the load at a given return frequency criteria – as illustrated below in Figure 7 and Figure 8. Instead of using the 3 different levels from the individual locations in Figure 4 (left), the FLACS viewer can take care of the 3D plot by itself either in a 3D volume representation (Figure 7) or using 2D cut planes in the geometry (Figure 8) (projected values on surfaces are also available but are less readable for the particular outcome of drag). These illustrations can immediately be compared all together and show immediate match. The high load regions are observed at the same locations. The major part of the module is experiencing a DAL for drag loads below 75 mbarg. The areas outside the module where the explosion venting occurs are exposed (which wasn’t accessible previously as monitoring points were not located at this particular place). The complementary Figure 9 is helpful as well to identify areas with low risk for a given exposure level.

Bearing in mind that this is an interactive Graphical User Interface, one can navigate into the module and observe in details specific locations of interest bringing a significant improvement in reporting. In the future (prospective), the processing of the results could even be more interactive using applications where vessels, piping, blast walls, objects... are tagged in the model and connected to the simulation result database.

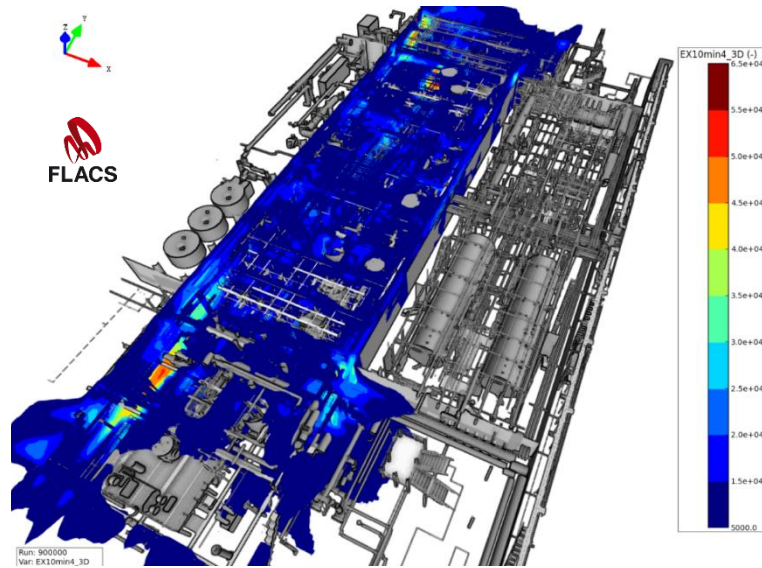


Figure 7: 3D volume plot in FLACS of the spatial DAL for drag loads (10^{-4} pr. year) for the studied deck

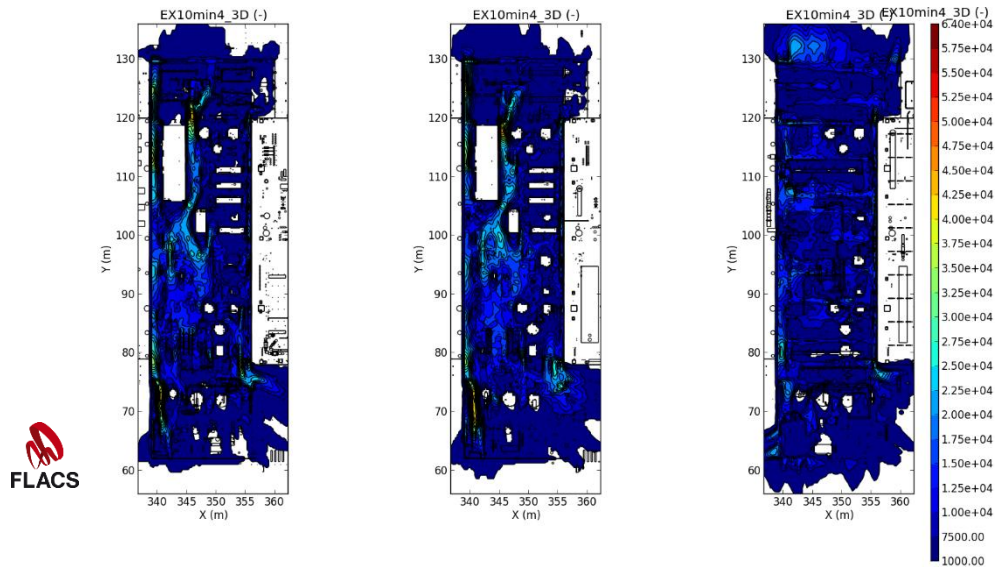


Figure 8: 2D cut planes in FLACS of the spatial DAL for drag loads (10^{-4} pr. year) for the studied deck

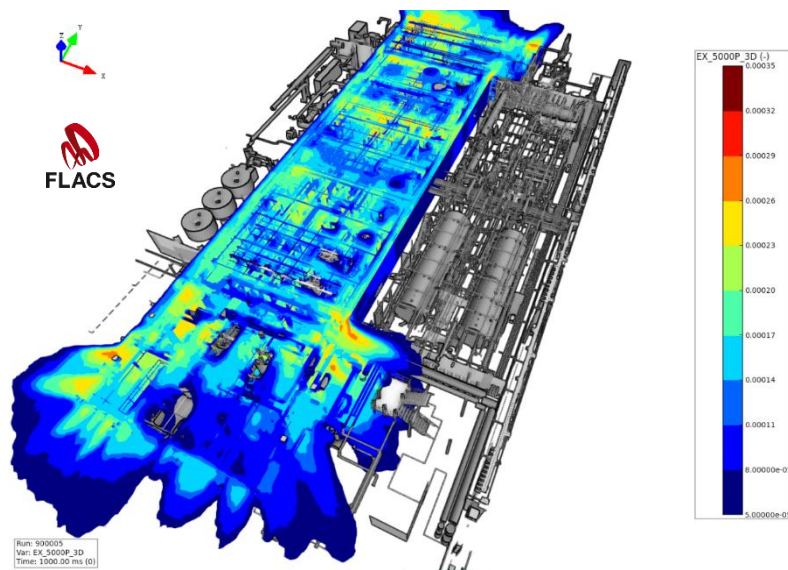


Figure 9: 3D plot in FLACS of frequency of exceedance of a given drag load (50 mbarg) for the studied deck

Directional dependency

In a second stage, the analysis highlights the high directional dependency of the loading. As a basis for Figure 5, exceedance curves are elaborated for the directional components of the absolute drag described at a given elevation using a 10^{-4} pr. year DAL criteria at each individual locations for the relevant directional drag.

The loading in the vertical direction (+/-Z, DRAG_z) is virtually negligible in all areas. The average values per elevation are systematically below 15 mbarg.

The loading in the direction transverse to the module (+/-X, DRAG_x) is highly irregular, showing values close to 0 on the boundary layers close to the side segregation wall (no cross flows) and more significant values in the “middle” of the module (expansion flows). Still the maximum value in the X-direction is close to 0.25 barg, south-east side, i.e. ~ 1/3 of the maximum value. Average value over the 3 elevations is ~ 30 mbarg.

The main contributor to the loading is clearly along the Y-direction (DRAG_y), i.e. the module main axis where the maximum value is retrieved. For most of the module, DRAG_y makes up for about 50 % of the absolute DAL for drag and for 80 % in a very large proportion of the geometry.

Figure 5, Figure 7 and Figure 8 are providing quantified values that are more suitable for further engineering. This way of presenting the drag loading echoes with the precepts used for “clever” engineering against drag loads: piping is preferentially routed along the main axis of such enclosed module to limit the constraints to X- and Z- axis loadings; areas with low directional drag are identified. Together with spatial differentiation, the gains in terms of design optimization are significant:

- As a general outcome, the understanding of the map of the risk related to drag is significantly increased, and can easily be interpreted thanks to the visualization.
- a 1:30 span between the maximum and the minimum values of absolute DAL for drag is observed when individual locations are studied;
- The prevailing loading is mainly along a single axis, the Y-axis, due to the specific tunnel shape of the deck;
- The particular case of the area located at the 5th line x 6th row at 1 m elevation is interesting and representative of a more open behaviour as the maximum value extracted from the spatial dependency (0.42 barg) is spread homogeneously between the X-axis (0.24 barg) and the Y-axis (0.21 barg);
- Supports and anchors can be designed to lower loading;
- Other load directions can also be applied comparing the ratio between the absolute value and the projected ones (e.g.: south-east region at the open edge of the firewall)...

As far as technically possible, this enables direct engineering recommendations to reduce the exposure to drag for small items. In any case, the results presented in Figure 5 and Figure 7 allow any kind of detailed approach for the response assessment as no simplification is included. It is suggested to use the spatial and directional reporting for drag as a standard for reporting results from explosion risk analysis.

Benefits, further work, interface with piping/structure disciplines, how to use the results

The presented method leads to a substantial improvement in the level of detail and of applicability when defining design loads. It supports solid basis for improving and optimising design. In general, reporting with the maximum possible accuracy would be highly beneficial to reduce the level of conservatism. In practice, when fitting a new skids or drag sensitive equipment in existing facilities, this way of reporting brings insight and support adequate qualitative decision making and engineering judgment. Obviously results may be affected by modification of the geometry, but at a first stage, one can expect that it will be sufficient for qualitative assessment. Although less practical than a “single value”, low extra efforts are likely to achieve a similar degree of safety at significant lower costs and will give more practicality in complying with safe design requirements.

Nevertheless, as drag loading is affected by congestion level and confinement, one should pay attention to accuracy of the geometry modelling. One should also maintain a holistic vision when analysing the spatial drag load patterns, e.g. in design stage, when geometry is likely to affect drag. When this approach is used for existing facilities to fit new skids or piping, there will be a certain level of new equipment that may require rerunning the analysis as large change in the geometry may affect explosion loads in general and spatial distribution of drag in particular. Also, the results are sensitive to the number of explosion simulations and in particular the number of cloud positions. A preliminary recommendation is that the explosion analysis of a conventionally sized offshore module should at least encompass ~100 explosion simulations covering the entire range of gas cloud sizes and locations as well as ignition points. As long as spatial accuracy is the main focus, the number of simulations itself can be increased in order to make sure that the results are not affected by the assumptions.

Once a good understanding of the potentials for load refinement is available, the key point is how these results will be efficiently used in the response calculations. Piping supports are not designed using a standardised methodology and various different assumptions are embedded in the tools and codes used; hence, it is stressed that an iterative process between safety and the structural / piping engineers might be useful to ensure a streamlined workflow. Depending on the specified approach to calculate the reaction forces and design the supports of a given pipe at a given location, the different expressions of the DAL for drag loads (maximum absolute drag, transient drag (t), directional DRAG_{x, y, z} components, DLF when it comes to time dependency, ...) can be used with more or less adaptations to derive the expression of the local force(s). In any case, this will reduce the level of conservatism, more or less. The key point is rather the “optimal” use of the available input depending on the methodology used for the response calculations. Consistency and proper documentation will be mandatory to maintain understanding during the life of the installation. Eventually, fundamental aspects will still need to be clarified by the risk-owner in terms of methodology to avoid over-design and optimize the interface between load definition and response calculations: avoid adding up maximum loads that originates from independent explosion cases; consider spatial dependency from a realistic explosion case: one part of the pipe might experience high loads while the opposite part far apart won't be

affected; consider phasing of the loading as the maximum local loads will not apply on the pipe sections at the same time... are examples of topics driven by company internal policies.

Obviously, using CFD, it will also be possible to perform direct coupling and map the load history in order to subsequently perform dynamic response calculations. However, for time and cost effective simplified response calculation methods, the current paper aims at providing the foundations to align the response calculations with the “most detailed” available input in terms of loading.

Conclusion

Proper definition of design load are a major topic in new builds or modification projects. For these, CFD explosion analyses are commonly performed as part of the QRA. Hence, in most projects the information required for refining DAL for drag loads are easily available with no or little extra work. In addition, a major improvement in the reporting is supported by the latest developments in FLACS, showing location-dependant risk-based results directly in the geometric model of the installation.

Considering the particular illustrative case of an offshore module where drag loads are originally reported to be high, the current report explores the possibilities, requirements and benefits from presenting the dimensioning drag loads according to the spatial dependency as well as the directional component. Compared to the common approach presenting a “single value” per deck, the large span in dimensioning drag values is demonstrated. It is demonstrated that the maximum value is experienced locally in the module. For such a particular “tunnel-shaped” module, it is highlighted that drag DAL contributions along the 3 spatial axis are highly inhomogeneous and, as it can be expected, the prevailing loading direction is along the main module axis.

When using an approach with high spatial accuracy, it is observed that high loads are only occur in a small area. The maximum value reported as per the commonly accepted approach is observed over a region corresponding to ~ 2.5 % of the total volume of the module. Reported local values at individual locations are mostly below 50 % of this maximum value. The required strength of the supporting structures is consequently significantly reduced in a large portion of the module, for a safe equivalent design in terms of prevention of escalation. Combining the directional dependency of the loading, it is illustrated that some regions of the module are mostly loaded along one prevalent direction meaning that a wise routing of the piping (along the same direction) could almost dissipate the drag constrains. This observation is specific to the studied module due to its tunnel shape. For the regions where this is not the case, it is illustrated how the absolute value is then distributed along the spatial axis and how constraints are again reduced. The new presentation of the results also allows defining loadings that deviate from the x, y and z directions if the response assessment would cover it. Even though less practical for design, this clearly illustrates the level of inherent conservatism included in the existing assessment.

The presented methodology will allow for substantial improvements of blast resistant design with significant cost and weight benefits as excessive design requirement in low exposure areas are avoided. In installations where high drag loads are calculated, refining of DAL for drag is likely to achieve an equally safe design at lower cost.

The methodology also present drag loading results in a format that can be used in a practical design setting. The designing engineer can, based on the provided load distribution map, chose to route ping or place sensitive equipment in areas where drag loads are low. And by doing so, he can take account of lower design load requirements. This is a fundamental improvement to the conventional “one value per deck” approach which provide very little guidance on possible design improvements. The secondary effect may include less structural steel and pipe supports, thereby reducing the congestion level and the explosion loads.

Emphasize is put on the need of a clear streamlined workflow between engineering disciplines to align the relevance of supplied results/output and its application in response assessment / design performed by the piping or structural engineers.

Practicality of the reporting is demonstrated using a new feature from the CFD tool FLACS: spatial risk exposure levels are directly reported in the geometrical model.

For assessment phase of existing installations, the new way of reporting is proposed as a standard approach.

References

- Baker, C. W. K. & S., 1983. *Explosion Hazards and Evaluation*. s.l.:Elsevier Scientific Publishing Company.
- Davis, S. et al., 2011. *Benefits of risk-based design through probabilistic consequence modeling*. Chicago, IL.
- FABIG, 2005. *Technical Note 8, Protection of Piping Systems subject to Fires & Explosions*, Ascot: Steel Construction Institute (SCI).
- Hansen, O., Gavelli, F., Davis, S. & Middha, P., May 2013. *Equivalent cloud methods for explosion risk and consequence studies*. *J. of Loss Prevention in the Process Industry*, 26(3), p. 511–527.
- ISO 19901-3, 2010. *Petroleum and natural gas industries - Specific requirements for offshore structures - Part 3: Topsides structure*, the International Organization for Standardization, s.l.: s.n.
- NORSOK Z-013, 2010. *Risk and emergency preparedness assessment*. s.l.:Norsok Standard; Available from Standard Norge, Postboks 242, N-1326 Lysaker, Norway.